Entropic rigidity of randomly diluted two- and three-dimensional networks

M. Plischke and D. C. Vernon
Department of Physics, Simon Fraser University, Burnaby, British Columbia, Canada V5A 1S6

B. Joós and Z. Zhou
Department of Physics, University of Ottawa, 150 Louis Pasteur, Ottawa, Ontario, Canada K1N 6N5

(Received 4 March 1999)

In recent work, we presented evidence that site-diluted triangular central-force networks, at finite temperatures, have a nonzero shear modulus for all concentrations of particles above the geometric percolation concentration p_c. This is in contrast to the zero-temperature case where the (energetic) shear modulus vanishes at a concentration of particles $p_r > p_c$. In the present paper we report on analogous simulations of bond-diluted triangular lattices, site-diluted square lattices, and site-diluted simple-cubic lattices. We again find that these systems are rigid for all $p > p_c$ and that near p_c the shear modulus $\mu \sim (p - p_c)^f$, where the exponent $f \approx 1.3$ for two-dimensional lattices and $f \approx 2$ for the simple-cubic case. These results support the conjecture of de Gennes that the diluted central-force network is in the same universality class as the random resistor network. We present approximate renormalization group calculations that also lead to this conclusion.
[S1063-651X(99)07109-3]

PACS number(s): 82.20.Mj, 05.70.Fh, 64.60.Cn

I. INTRODUCTION

Since the pioneering work of Feng and Sen [1] it has become clear that, upon dilution at $T=0$, a network of particles interacting only through central two-body forces generically loses its ability to withstand shear at a concentration p_r of particles that is higher than the geometric percolation concentration p_c at which a spanning cluster first appears [2–4]. This phenomenon of rigidity percolation is now quite well understood. However, recent work [5,6] has shown that for $T \neq 0$ there is a contribution to the shear modulus that is entropic in origin and which persists to $p = p_c$. Conceptually this result is easy to understand by analogy with the physics of rubber elasticity — another primarily entropic phenomenon: Near percolation, diluted lattices are composed essentially of long chains of singly connected particles linked to each other at various junction points. These chains are the direct analog of the polymer chains that are crosslinked in rubber to create a rigid amorphous material. When the distance between junction points or crosslinks is changed upon deformation of the sample, the entropy is generically decreased, resulting in an increase of free energy and a restoring force. As soon as a sample percolates, there is a net shear restoring force. The connecting chain of particles acts as a stretched spring.

Although this picture seems quite straightforward, there are a number of interesting open questions about entropic elasticity. The first has a long history, dating back to the work of de Gennes [7]. He argued, on the basis of a simple analogy between Kirchhoff's laws for resistor networks and the force balance conditions for networks of springs, that the random resistor networks and diluted networks of springs should be in the same universality class. More precisely, if the conductivity σ of a diluted network of resistors vanishes at the geometric percolation point as $\sigma \sim (p - p_c)^t$ and the shear modulus of a central-force network $\mu \sim (p - p_c)^f$ then the prediction is $f = t$. Our earlier results [5] were consistent with this prediction but certainly could not rule out a small discrepancy. Moreover, for dimensionality $d=2$, $t \approx \nu$ where ν is the percolation correlation length exponent so that the data do not distinguish between the possibilities $f = \nu$ and $f = t$. We note that this is in striking contrast to the zero-temperature result, where the exponent that describes the behavior of μ near p_r is quite different from t [8].

In this article we continue our investigation of diluted central-force networks. We report on molecular dynamics simulations of site-diluted square lattices and bond-diluted triangular lattices. The choice of these two systems was motivated by a desire to reduce crossover effects. On the triangular lattice, rigidity percolation occurs for $p_r \approx 0.6975$ (site dilution) and $p_r \approx 0.66$ (bond dilution) whereas geometric percolation occurs at $p_c = 0.5$ (site) and $p_c = 2 \sin \pi/18 \approx 0.3473$ (bond). The range of concentration over which rigidity is entropic is therefore much greater for bond dilution than for site dilution and one might expect that the data would be less influenced by the proximity of the rigidity percolation critical point. This effect is even more pronounced on the square lattice: The energy of a square network is unchanged by an infinitesimal simple shear, i.e., $p_r = 1.0$. Therefore, over the entire range of concentrations $1 \geqslant p > p_c \approx 0.592\,77$ [9] a nonzero shear modulus is due to entropy.

Since these systems are two dimensional, they also have the property $t \approx \nu$ and therefore the present simulations are again unable to distinguish between the aforementioned potential exponent equalities $f = \nu$ and $f = t$. Partly because of this ambiguity, we have also carried out molecular dynamics (MD) simulations for diluted simple-cubic lattices. In three dimensions, $\nu \approx 0.879$ [10] whereas $t \approx 2.0$ [11]. Therefore, it should be possible to rule out one of the aforementioned exponent equalities. As well, the simple-cubic lattice shares with the square lattice the property $p_r = 1.0$ and there is therefore a considerable range of concentrations $1.0 \geqslant p > p_c \approx 0.31$ over which rigidity is entropic in origin.

Since simulations of relatively small systems are incapable of producing unambiguous conclusions on issues such as universality classes, we have also carried out renormalization group calculations on a number of regular fractals. These structures are designed to model the geometry of the backbone of the percolating cluster near p_c [12–14]. All of these calculations support the conclusion $f=t$.

The structure of this article is as follows. In Sec. II we describe the models and computational procedures. Results of the simulations are presented in Sec. III and a description of the renormalization group calculations follows in Sec. IV. Several experiments done on disordered materials are discussed in Sec. V. We conclude with a brief discussion and outlook for future work in Sec. VI.

II. MODEL AND COMPUTATIONAL METHODS

The three systems simulated consist of particles tethered to each other through the potential energy

$$V(r_{ij})=\frac{1}{2}k[|\mathbf{r}_i-\mathbf{r}_j|-r_0]^2, \tag{2.1}$$

where, in the undiluted case $p=1$, the vertices i, j label nearest neighbor sites on a square, triangular, or simple-cubic lattice with equilibrium spacing of r_0. In the site-diluted system at concentration p only the remaining nearest neighbor pairs interact with potential energy (2.1); bond dilution implies setting a fraction of the nearest neighbor interactions to zero. Since only nearest neighbors interact, and there are no hard core repulsions, these models are (in the two-dimensional case) *phantom* rather than *self-avoiding* membranes in the language used to describe tethered membranes [15]. The implication is that, even with only two degrees of freedom per particle, these systems would crumple in order to increase their configurational entropy if the boundaries of the nets were not fixed [16]. This is relevant because it implies that even an undiluted square net, with every particle at its ground state position, is effectively under entropic tension when $T\neq 0$. It is well known that square lattices under tension (at $T=0$) have a nonzero shear modulus [17] whereas at zero tension they are soft. Thus it is not surprising that our finite-temperature simulations yield a nontrivial shear modulus for both diluted and undiluted square lattices.

To obtain the shear modulus, we have carried out molecular dynamics simulations for both systems. For the triangular networks, we imposed a pure shear deformation $L_x\rightarrow(1+\epsilon)L_x$, $L_y\rightarrow(1-\epsilon)L_y$ on the computational box. This transformation preserves the area of the cell to first order in ϵ and within linear elasticity theory for isotropic materials, the shear modulus is given by

$$\mu=\frac{p_{xx}-p_{yy}}{4\epsilon}. \tag{2.2}$$

Here p_{xx} and p_{yy} are the diagonal elements of the pressure tensor which are easily calculated in a MD simulation using the virial theorem. In practice, we have taken both positive and negative values $\epsilon=\pm 0.005$ for each sample and averaged the results over both simulations. Periodic boundary

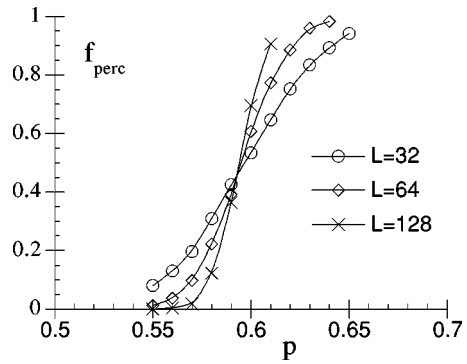

FIG. 1. Probability $f_{\mathrm{perc}}(p)$ that the largest cluster percolates in both directions on site-diluted square lattices as a function of occupation probability p. The lines are a guide to the eye. The three curves intersect very close to the percolation probability $p_c=0.592\,77\ldots$.

conditions were used throughout and as an initial condition, all particles were affinely displaced from their equilibrium positions. The bulk of these constant energy simulations were carried out for mean temperatures of both $T=0.005kr_0^2/k_B$ and $T=0.001kr_0^2/k_B$ for pL^2 particles with L ranging from 16 to 128 and p in the entropic regime $0.66>p>0.3473$. For a given p, the fluctuations from sample to sample of the shear modulus are very substantial and it proved necessary to average over many realizations to obtain well-converged results. For the smallest ($L=16$) samples, and the lowest p, 60 realizations averaged over both positive and negative shears were used, while for the larger samples at high p, as few as ten realizations were required.

Since systems with the symmetry of the square or simple-cubic lattice are not isotropic solids, the elastic constant governing the pure shear deformation used above is not the shear modulus — the symmetry of a square does not require these elastic constants to be equal. For these systems, we have instead imposed a simple shear deformation by shifting the boundaries of the computational box to $x_{\min}(y)=\epsilon y$, $x_{\max}(y)=\epsilon y+Lr_0$ where the undeformed box is a square of size $Lr_0\times Lr_0$ or cube of volume $(Lr_0)^3$. In this case, the shear modulus is given by

$$\mu=\frac{[p_{xy}(\epsilon)-p_{xy}(0)]}{\epsilon}, \tag{2.3}$$

where p_{xy} is the off-diagonal element of the pressure tensor. In this equation, we have subtracted $p_{xy}(0)$, which represents the frozen stresses for a given realization of the disorder. Clearly, this quantity is zero by symmetry for $p=1$ and should average to zero even for diluted lattices. However, for a finite number of samples, convergence is much more rapid if these frozen stresses are subtracted sample by sample. For these systems, we carried out Brownian MD [18], primarily at a temperature $T=0.01kr_0^2/k_B$ with a time step $\delta t=0.016\sqrt{k/m}$ and a deformation parameter $\epsilon=0.05$ which is still in the linear regime. For the square lattice, the samples ranged in size from $L=16$ to $L=128$ and concentrations from $p=1$ to $p=0.595$. For the simple-cubic lattice, we were able to simulate systems of size $8\leqslant L\leqslant 32$ for concentrations $0.315\leqslant p\leqslant 1.0$. In the next section, we describe the results obtained.

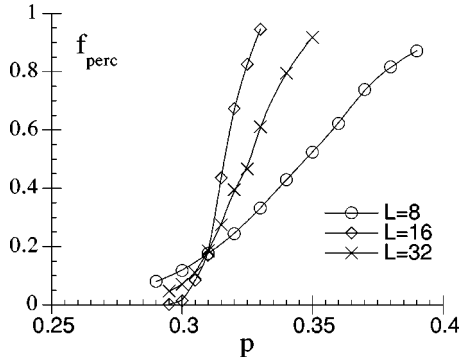

FIG. 2. Probability that the largest cluster percolates in all three directions on site-diluted cubic lattices. We estimate that $p_c \approx 0.310$.

It is interesting to note that if the shear modulus is entirely of entropic origin, as we expect it to be in the square lattice following the arguments given at the beginning of this section, then $\mu = p_{xx}$. Within computational error, we have observed this to be the case for p close to the percolation threshold.

III. RESULTS

For systems of the size that we are able to simulate, finite-size effects are quite important. This is illustrated in Figs. 1 and 2 where we have plotted the probability $f_{\text{perc}}(p)$ that a spanning cluster exists as a function of the site occupation probability for square and simple-cubic lattices. In the thermodynamic limit, this function is a step function $f_{\text{perc}}(p) = \theta(p - p_c)$ and its departure from that form is an indicator of the extent of finite-size effects.

In Fig. 3 we show the raw data for the shear modulus as a function of p for the bond-diluted triangular lattice, and in Figs. 4 and 5 we show the same data for site-diluted square and simple-cubic lattices. The finite-size effects are clearly evident, especially for $p \approx p_c$. The reader might wonder whether $\mu(p, L \to \infty) \to 0$. As in the case of the site-diluted triangular lattice [5], the data when plotted as a function of L^{-1} clearly show a finite intercept at $L^{-1} = 0$ for all $p > p_c$.

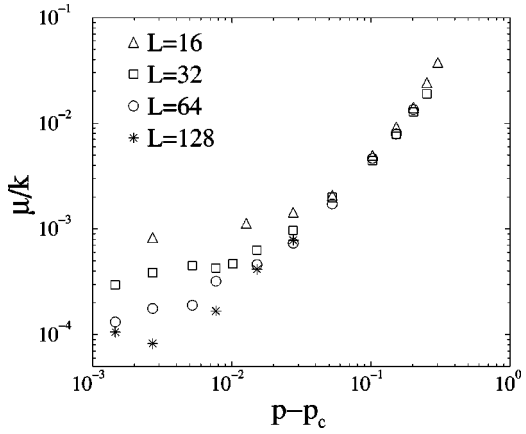

FIG. 3. Shear modulus as a function of p for bond-diluted triangular lattices and $16 \leqslant L \leqslant 128$. The simulations for this data were done at a mean temperature of $T = 0.005 k r_0^2 / k_B$.

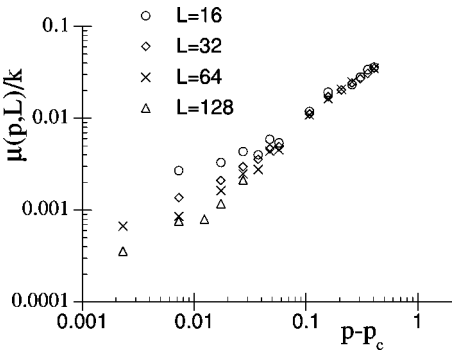

FIG. 4. Shear modulus as a function of p for site-diluted square lattices and $16 \leqslant L \leqslant 128$.

As mentioned in the Introduction, the shear modulus of two-dimensional randomly diluted networks behaves as $\mu(p,T) \sim (p - p_c)^f$ with $f \approx 1.3$, a value that is close to both ν (4/3) and the conductivity exponent t (1.3). A rough estimate of the exponent f in three dimensions can be obtained by fitting the raw data to the form $\mu = a(p - p_c)^f$ with a and f fitting parameters. For the simple-cubic lattice, we take $p_c = 0.31$, the value obtained from the intersection of the curves in Fig. 2. This type of fit yields estimates of the exponent $f = 2.0 \pm 0.2$ when the data for $L = 16$ and $L = 32$ are used. The solid line in Fig. 5 is a plot of $(p - p_c)^2$ and it is clear that the data are consistent with this functional form.

For the case of the two-dimensional lattices, it is necessary to carry out a finite-size scaling analysis to obtain a reasonably accurate estimate of the exponents. The finite-size scaling ansatz reads

$$\mu(p,L) = L^{-f/\nu} \Phi(L/\xi(p)) = L^{-f/\nu} \tilde{\Phi}(L(p - p_c)^{\nu}), \tag{3.1}$$

where the scaling function $\tilde{\Phi}(x) \sim x^{f/\nu}$ for $x \gg 1$ and $\tilde{\Phi}(x) \to \text{const}$ as $x \to 0$. In this expression, p_c is taken to be the percolation concentration of the infinite system. If this ansatz holds, a plot of $L^{f/\nu}\mu$ as a function of $L(p - p_c)^{\nu}$ should produce a collapse of the data for different values of L. Such plots are shown in Figs. 6–8 for the three systems investigated here. In all three cases we obtain a very respectable collapse of the data. Although all three data sets have considerable error bars associated with the estimates of μ there are no clearly discernible trends and we conclude that in the thermodynamic limit $\mu \sim (p - p_c)^f$ with $f \approx 1.33$ in two di-

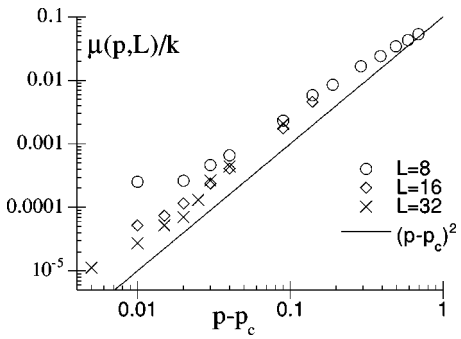

FIG. 5. Shear modulus as a function of p for site-diluted simple-cubic lattices and $8 \leqslant L \leqslant 32$.

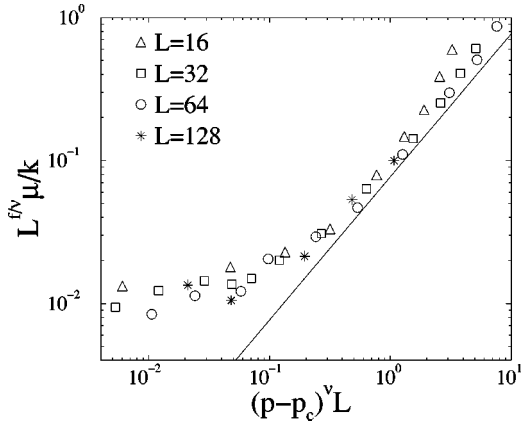

FIG. 6. Finite-size scaling plot of the data of Fig. 3. Here we have used $\nu=4/3$, $p_c=0.347\,30$, and $f=\nu$.

mensions and $f\approx 2.0$ in three dimensions. The deviation of the data for $L=16$ in Fig. 6 from a straight line at high p is due to the crossover to the energetically rigid region, which begins at $p_r\approx 0.66$. The last point in the $L=16$ data corresponds to $p=0.65$, almost at the critical point, and some realizations of the diluted lattice have significant rigid regions at lower p, resulting in the increase in shear modulus observed. There is no energetically rigid region in either the square or simple-cubic lattice, so this effect does not appear.

To remove the effects of the energetic rigidity in the triangular lattice, we plot the entropic contribution to the shear modulus in Fig. 9. This is given by [6]

$$\mu_s = T\left(\frac{\partial \mu}{\partial T}\right)_{p,L}. \tag{3.2}$$

The higher p values of the $L=16$ data now fall closer to the other data, as expected.

Our data are therefore consistent with the conjecture of de Gennes [7] that the random resistor network and the diluted central-force network are in the same universality class — a marked contrast to the behavior of the zero-temperature rigidity near the rigidity percolation point. In the next section we provide further evidence for this conclusion by constructing a renormalization group transformation for two-dimensional networks.

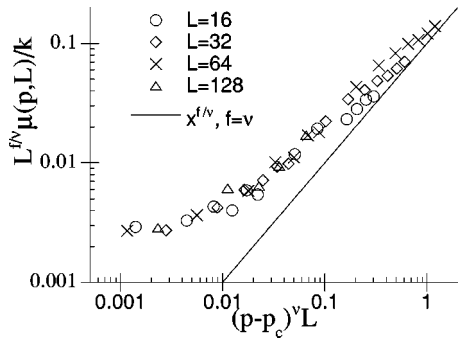

FIG. 7. Finite-size scaling plot of the data of Fig. 4. Here we have used $\nu=4/3$, $p_c=0.592\,77$, and $f=\nu$. The solid line is a plot of $[(p-p_c)L]^{f/\nu}$ for $L=32$.

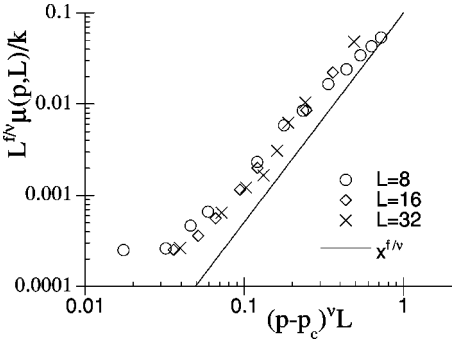

FIG. 8. Finite-size scaling plot for the simple-cubic lattice with $p_c=0.31$, $\nu=0.879$, and $f=2.0$. The solid line shows the expected asymptotic form of the scaling function.

IV. RENORMALIZATION GROUP

There have been a number of approximate renormalization group (RG) calculations for random resistor networks near the percolation point. Early work by Stinchcombe and Watson [19] and Bernasconi [20] was based on real space RG transformations for small finite clusters. These approaches produced two recursion relations, one for the probability p that a renormalized bond would be occupied and one for the distribution of conductivities $P(\sigma)$. Thus, one obtains both the correlation length exponent ν and the conductivity exponent t, both to respectable accuracy [20]. Later, a different approach was developed based on the idea that the geometry of the system at percolation can be modeled quite accurately by a regular fractal, such as a Sierpinski gasket [12], modified Koch curve [13], or other hierarchical lattices [14]. Since these hierarchical lattices are expected to be relevant only at the percolation point, there is no recursion relation for the probability p and generically only a linear relation between σ' and σ. Using the value of the (presumed known) correlation length exponent ν, one can then calculate the exponent t. In $d=2$, one obtains a best estimate $t\approx 1.322$ [14], in very good agreement with Monte Carlo simulations.

If one replaces the resistors on the network with a set of *Gaussian* springs, i.e., springs with Hamiltonian

$$\mathcal{H}(i,j)=\beta H = K\{\mathbf{r}_i-\mathbf{r}_j\}^2 \tag{4.1}$$

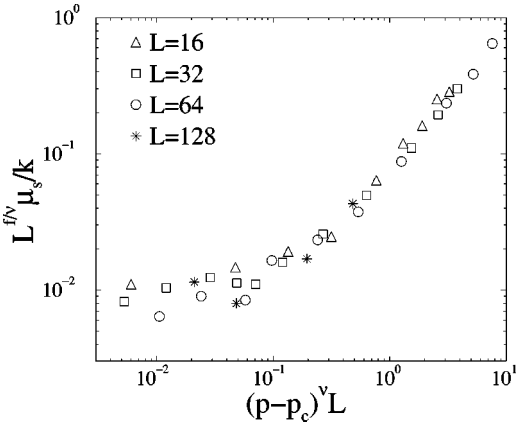

FIG. 9. Finite-size scaling plot of the entropic contribution to the shear modulus of a bond-diluted triangular lattice, in arbitrary units.

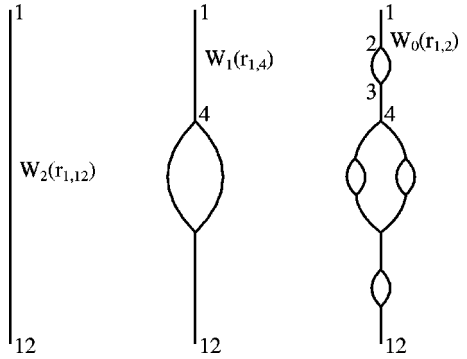

FIG. 10. Three generations of the hierarchical lattice of [14].

between any pair of sites connected by a resistor, one can produce a renormalized value of (distribution for) K by integrating out some of the $\mathbf{r}_i$'s. This recursion relation is exactly the same as the recursion relation for the conductivities, i.e., we arrive at de Gennes's conclusion [7] by a different route. However, the technical flaw in de Gennes's argument is that it breaks down for arbitrary central-force fields. For a general potential energy $V(r_{ij})$, including Eq. (2.1), the equations of motion do not separate and the formal equivalence between Kirchhoff's laws and mechanical equilibrium is lost.

Because of this difficulty, we have examined how the non-Gaussian Hamiltonian (2.1) varies under renormalization for some of the regular fractals mentioned above. Here we report results only for the hierarchical lattice of Ref. [14] which is sketched in Fig. 10. We define $W_0(r_{ij}) = \exp\{-\mathcal{H}_0(r_{ij})\}$ where

$$\mathcal{H}_0(r_{ij}) = \beta V(r_{ij}) = K[|\mathbf{r}_i - \mathbf{r}_j| - r_0]^2, \tag{4.2}$$

where we take $r_0 = 1$ and $K = 1$ and where i, j are any pair of nearest neighbor vertices on the highest generation of the hierarchical lattice. Integrating over $\mathbf{r}_2$, $\mathbf{r}_3$, and the other coordinates at the ends of the smallest loops in the highest generation produces the next highest generation with a Boltzmann weight $W_1 = \exp\{-\mathcal{H}_1\}$ describing the interaction between the remaining particles. This procedure can clearly be continued indefinitely. However, as is evident from Fig. 11, one step is sufficient. In this figure, we show the results of a single such numerical integration. Plotted together with $W_0(r)$ is $W_1(r)$, normalized to unity at $r = 0$. The striking feature of these curves is that the equilibrium length scale $r_0 = 1$ of the starting Hamiltonian has completely disappeared: The solid curve is a fit of the function W_1 to a Gaussian peaked at $r = 0$. The fit is essentially perfect, leading to

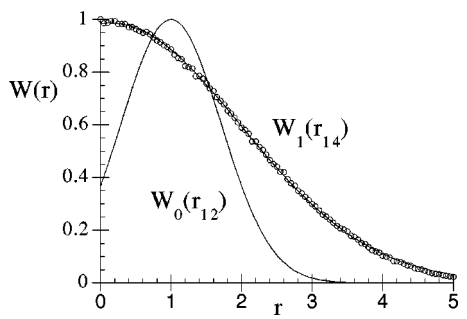

FIG. 11. One step in the renormalization of the Hamiltonian $\mathcal{H}_0$.

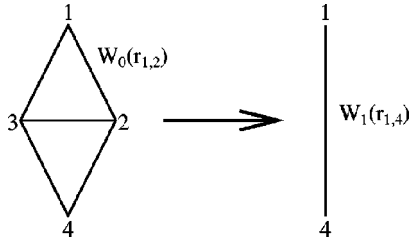

FIG. 12. Multiply connected cluster used in the real space renormalization group calculation of Ref. [20].

the conjecture that a general central-force potential, on this hierarchical lattice, under renormalization iterates toward the Hamiltonian (4.1) and therefore that the rigidity problem at finite T and the random resistor problem are indeed in the same universality class. The same results are obtained for the other regular fractals mentioned above.

It is interesting to carry out a similar calculation for clusters that are more characteristic of diluted lattices *above* the rigidity percolation point. In Fig. 12 we show one of the bond configurations that occurs in the real space RG calculation of Ref. [20]. Integrating out the coordinates $\mathbf{r}_2$ and $\mathbf{r}_3$ in W_0, we obtain the renormalized Boltzmann weight $W_1(\mathbf{r}_{14})$. This is shown in Fig. 13 together with $W_0(r)$ for $K = k/2k_BT = 5.0$. What is notable is the appearance of a secondary peak at $r_1 = \sqrt{3}r_0$. The two peaks are due to the fact that the set of springs with the topology shown has two possible configurations with all lengths equal. The first, shown in Fig. 12, has vertices 1 and 4 separated by $\sqrt{3}r_0$. However, the configuration in which vertex 4 is on top of vertex 1 also has all spring lengths equal. The peak at $r_1 = 0$ is due to this configuration. As T is lowered or K increased, the second peak becomes more pronounced, and at zero temperature contains the entire Boltzmann weight: The phase space for the problem separates into two regions corresponding to the two configurations of the set of springs, and if the system starts in the extended configuration, it must remain in it. Our interpretation is that at zero temperature, for $p > p_r$, the flow in a RG transformation is toward $p = 1$ where structures such as that of Fig. 12 dominate. At the same time, the characteristic length r_0 which represents the ground state lattice constant flows toward br_0 where b is the change in length scale due to the RG transformation [21].

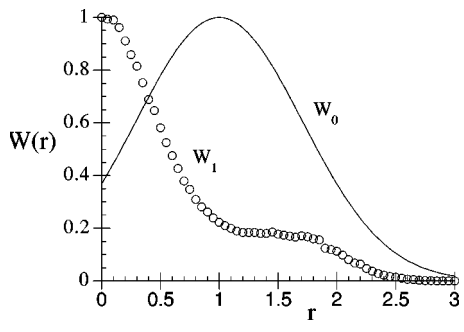

FIG. 13. Original Boltzmann weight W_0 and renormalized weight W_1 for the transformation of Fig. 9.

V. EXPERIMENTS

A number of experiments have been done to measure the elastic moduli of different amorphous solids, with varying results. All of these experiments are done with three-dimensional samples and therefore the prediction that the exponent $f \approx 2.0$ is what is being tested.

The best agreement with the predictions discussed here is found in an experiment done on a gel formed from tetraethoxysilane (TEOS) in a solution of water and ethanol [22]. These authors found $f = 2.0 \pm 0.1$, as well as other exponents reasonably close to those of conductivity percolation. These exponents were found only close to the gelation point; far from this point, a crossover to the vector elasticity exponents was seen. In this experiment, the time from the gelation transition was measured, and p was taken to be proportional to this time. This assumption is supported by another experiment showing that the degree of condensation is proportional to time near the gelation transition [23].

This good agreement is encouraging as the silica gel studied is a soft material, where the entropic effects are likely to be important. Also, the gelation transition and the structure of the gel are reasonably well described by percolation theory.

Another experiment, done on a porous ceramic material [24], also found reasonable agreement with our predictions. In this experiment, the conductivity and elastic exponents of a set of porous ceramics of lead zirconate-titanate prepared by tape casting and sintering were determined. Since both conductivity and elastic exponents were measured, the analogy between the two can be tested in the same material. The conductivity and Young's modulus were measured as a function of the volume fraction v, which is taken to correspond to p in the percolation problem. The conductivity exponent t was found to be 2.27 ± 0.25, and the elastic exponent was $f = 2.2 \pm 0.2$. The fact that the conductivity and elasticity exponents are similar is encouraging, as is the fact that these quantities vanish at the same critical volume fraction.

VI. DISCUSSION

In this article we have presented compelling evidence that at nonzero temperature the shear modulus (and presumably other moduli) of diluted central-force networks remain finite for all concentrations above the geometric percolation concentration. This is true even for energetically soft lattices such as the square and simple-cubic lattices for which the rigidity percolation concentration is $p = 1$. Strictly speaking, rigidity percolation is therefore a $T = 0$ effect although considerable softening of the elastic constants near p_r does occur at finite temperature.

We have also presented evidence that the critical behavior of the moduli at the percolation point is the same as that of the conductivity of a random resistor network of the same dimensionality, thus lending support to a conjecture of de Gennes [7].

Central-force networks are somewhat special from an energetic perspective since the inclusion of bond-bending forces reduces the rigidity percolation point to the geometric percolation point. The exponent τ that characterizes the critical behavior of the elastic moduli (at $T = 0$) of systems with bond-bending forces is also known to be significantly larger than that of random resistor networks [8]. However, at finite temperatures we expect that these systems will have the same entropic contribution to the free energy as central-force networks. Since the exponent f that characterizes the behavior of entropic elasticity is smaller than τ we conjecture that entropic effects will dominate and that the behavior found in the calculations presented here is in fact general and independent of microscopic detail. However, this remains a subject for future investigation.

ACKNOWLEDGMENTS

We thank P.M. Duxbury, Paul Goldbart, and M.F. Thorpe for helpful discussions. This research was supported by the NSERC of Canada.

[1] S. Feng and P.N. Sen, Phys. Rev. Lett. **52**, 1891 (1984).
[2] S. Feng, M.F. Thorpe, and E. Garboczi, Phys. Rev. B **31**, 276 (1985).
[3] C. Moukarzel and P.M. Duxbury, Phys. Rev. Lett. **75**, 4055 (1995); D.J. Jacobs and M.F. Thorpe, Phys. Rev. E **53**, 3682 (1996).
[4] For some recent developments see *Rigidity Theory and Applications*, edited by M.F. Thorpe and P.M. Duxbury (Plenum Press, New York, 1998).
[5] M. Plischke and B. Joós, Phys. Rev. Lett. **80**, 4907 (1998).
[6] B. Joós, M. Plischke, D.C. Vernon, and Z. Zhou, in Ref. [4].
[7] P.G. de Gennes, J. Phys. (France) Lett. **37**, L1 (1976).
[8] S. Roux, J. Phys. A **19**, L351 (1986); M. Sahimi, J. Phys. C **19**, L79 (1986).
[9] T. Gebele, J. Phys. A **17**, L51 (1984).
[10] J. Adler, Y. Meir, A. Aharony, and A.B. Harris, Phys. Rev. B **41**, 9183 (1990).
[11] D. Stauffer and A. Aharony, *Introduction to Percolation Theory*, 2nd ed. (Taylor and Francis, London, 1992).
[12] Y. Gefen, A. Aharony, B.B. Mandelbrot, and S. Kirkpatrick, Phys. Rev. Lett. **47**, 1771 (1981).
[13] B.B. Mandelbrot and J.A. Given, Phys. Rev. Lett. **52**, 1853 (1984).
[14] L. de Arcangelis, S. Redner, and A. Coniglio, Phys. Rev. B **31**, 4725 (1985).
[15] Y. Kantor and D.R. Nelson, Phys. Rev. A **36**, 4020 (1987).
[16] The mean square radius of gyration of a phantom membrane grows with the stretched length L of an edge as $R_g^2 \sim \ln L$ rather than as L^2 for a self-avoiding membrane in two dimensions. See [15], and references therein.
[17] See, for example, S. Alexander, Phys. Rep. **296**, 65 (1998).
[18] M.P. Allen and D.J. Tildesley, *Computer Simulation of Liquids* (Oxford University Press, New York, 1987).
[19] R.B. Stinchcombe and B.P. Watson, J. Phys. C **9**, 3221 (1976).
[20] J. Bernasconi, Phys. Rev. B **18**, 2185 (1978).
[21] Similar renormalization group calculations have been carried

out by Y. Kantor, M. Kardar, and D.R. Nelson, Phys. Rev. A **35**, 3056 (1985) for self-avoiding tethered membranes. These authors also found that for $T \neq 0$ the renormalized Boltzmann weight W flows toward a Gaussian peaked at $r = 0$.

[22] F. Devreux, J.P. Boilot, F. Chaput, L. Malier, and M.A.V. Axelos, Phys. Rev. E **47**, 2689 (1993).

[23] L. Malier, J.P. Boilot, F. Chaput, and F. Devreux, Phys. Rev. A **46**, 959 (1992).

[24] F. Craciun, C. Galassi, and E. Roncari, Europhys. Lett. **41**, 55 (1998).